SURFTRAP - Development and Optimisation of a Process to Biosynthesize Reactive Iron Mineral Surfaces for Water Treatment Purposes

Peiffer S.*, Paikaray S., Damian Ch. (1), Janneck E., Ehinger S., Martin M. (2), Schlömann M., Wiacek C., Kipry J., (3), Schmahl W., Pentcheva R., Otte K., Götz A., Wang Z., Hsieh K. (4), Meyer J., Schöne G. (5), Koch T. (6), Ziegler A. (7), Burghardt D. (8)

(1) Department of Hydrology, University of Bayreuth, Universitätsstraße 30, D-95440 Bayreuth

(2) GEOS Ingenieurgesellschaft mbH, Gewerbepark »Schwarze Kiefern«, D-09633 Halsbrücke

(3) Department of Environmental Microbiology, Tech. University of Freiberg, Leipziger Str. 29, D-09599 Freiberg

(4) Department of Earth and Environmental Science, Section Crystallography, University of Munich, D-80333 Munich

(5) Wismut GmbH, 09117 Chemnitz

(6) Vattenfall Europe Mining AG, 03050 Cottbus

(7) Central Facility for Electron Microscopy, University of Ulm, 89069 Ulm, Germany

(8) Institute for Groundwater Management, Technical University of Dresden, 01062 Dresden

*Coordinator of the project

1. Introduction

In this project we aim to develop a low-cost technology to remove ionic constituents from raw waters such as arsenic species. The proposed technology is based on the reactivity of schwertmannite, an oxyhydroxosulfate of the mean stochiometry $Fe_8O_8(OH)_6SO_4$ (molar mass 772.89 g/mol). This mineral typically forms in acidic and sulfate rich mine waters as a secondary mineral upon oxidation of Fe(II) in a biologically mediated process. Schwertmannite can be generated in a biotechnological process after aeration of mining process waters. It forms surface-rich aggregates of needle-like nanocrystals. It rapidly transforms into ferric hydroxides of high specific surface area once exposed to water containing at least some alkalinity. Our rationale follows the concept to make use of this transformation reaction by adding biosynthesized schwertmannite to contaminated raw waters where it generates a large sorption capacity to remove the pollutants (*Peiffer et al., 2008*).

2. Materials and Methods

2.1. Microbial Investigations

2.1.1. Depth profile of activity of microorganisms in schwertmannite

A Schwertmannite core from the carrier material of the pilot plant was collected with a hollow drill and cutted into 0.5 cm layers (volume of each layer=1.7 cm^3). The mineral was dissolved with 0.2 M oxalic acid and the cells

Table1: 16S rRNA probes used for FISH analyses

Probe	Target	Probe sequence (5'-3')	Reference
BSC0459_deg	*Ferrovum myxofaciens*	TCCAGRTTATTCGCCTGA	modified by Hallberg et al., 2006
GALTS0084	*Gallionella* TrefC4	CCACTAACCTGGGAGCAA	Hallberg et al., 2006
Helper 1	Upstream of GALTS0084	GATATATTACTCACCCGTTCG	Hallberg et al., 2006
Helper 2	Downstream of GALTS0084	GCCCCCAGGCCCGTTCGA	Hallberg et al., 2006

were washed with 1x PBS buffer. The resuspended cells were analysed with the LIVE/DEAD® BacLight™ Bacterial Viability Kit (Invitrogen, L13152) and FISH (fluorescence in situ hybridisation). The FISH analyses were performed after *Hallberg et al.* (2006) with probes for Ferrovum myxofaciens and Gallionella TrefC4 (tab. 1).

2.1.2 Biologic Analysis / Interface Bacteria – Mineral

We investigated samples from cultures of the species *Leptospirillum ferrooxidans*. To investigate the interface between mineral and organic matter the organic matter had to be fixated. This was done by physical (high pressure cryo-fixation) and chemical methods (2.5 % glutardialdehyde/2.0 % paraformaldehyde mixture in 0.2 M cacodylate butter (pH 4.5)). Several steps for drying and contrasting followed. The fixated samples were embedded in Epon and cut into 70 nm thick sections with a DIATOM diamond knife on a microtome for the TEM. For the SEM work, the samples were critical point dried and coated with platinum. Samples were taken from two positions: from the sediment and from a bioactive TERMINOX foil.

2.2 Schwertmannit generation

The designed pilot plant consists of an oxidation basin with removable growth carriers as well as an aeration and a precipitation tank. The overall volume is about 10.5 m³ and the oxidation basin has a capacity of 8.14 m³. Due to the high flow rate of the circulation pump (approximately 30 m³/h) low gradients of process parameters can be guaranteed. The water inflow is intensively aerated. A chain cleaner assembled at the bottom of the oxidation basin removes dropping schwertmannite to the sludge colllecting channel. From there the sludge is pumped to a storage tank where the sludge can sediment and thicken. The thickened sludge can be recycled to the oxidation basin or pumped into big bags for dewatering by gravity.

From the chemical engineering point of view, the designed pilot plant is a hybrid type of bioreactor. It has physical characteristics of a fixed-bed reactor in parallel with a circulation reactor. The advantages of this special reactor design are avoiding plugs in the fixed-bed (growth carrier) and a free circulation inside the oxidation basin.

The pilot plant was operated continuously since the start of the project.

2.3. Mineralogical and Structural Analysis

2.3.1. Mineral analysis

The crystal structure of the prepared precipitates (see below) was examined by XRD. XRD measurements were performed on a Stoe powder diffractometer and on an Oxford Diffraction area detector diffractometer, both using Mo-kα_1 radiation. Scanning electron microscope (SEM) analyses of the biologic samples were performed with a Hitachi S-5200 field emission scanning electron microscope equipped with an EDX and a STEM detector. For the SE-pictures an accelerating voltage of 4kV was used and for the EDX and STEM analyses 20kV was employed. SEM pictures of the mineral samples were taken on a JEOL 6500 F SEM with 5kV accelerating voltage.

Specific surface areas were measured by Brunauer-Emmett-Teller (BET) method (*Brunauer et al., 1938*) using a FlowSorb II 2300 (Fa. Micromeritics) and N_2/Ar (80 %/20 %) as adsorbate.

Different methods from literature to produce schwertmannite were compared. The first method was published by *Bigham et al. 1990*: 2L of MilliQ water were heated to 60 °C and 10.8 g of $FeCl_3$*$6H_2O$ and 3 g of Na_2SO_4 were added. The solution was kept at 60 °C for 12 minutes. The orange suspension was then placed in a dialysis bag and dialyzed against MilliQ water. The water was changed daily during a period of 33 days. The precipitate was then filtered and vacuum dried. This sample will be referred to as dialyzed schwertmannite. A second recipe originates from Pentinghouse and was first published by *Regenspurg et al. 2004*: 5 g of $FeSO_4$ was dissolved in 1L of distilled water. Then 5 mL of H_2O_2 (32 %) were added. The solution became brown-red, and after only few minutes, a rust-colored precipitate could be observed. After 24 h of ripening in solution at 25 °C the obtained material was vacuum-

dried. We will refer to that material as fast-H_2O_2-schwertmannite. The method of Pentinghouse was also applied in a modified way. H_2O_2 (0.03%) was pumped over 24 h continuously (flow rate: 5 mL/h) to 100 mL culture media iFe containing 25 mM ferrous iron (*Johnson and Hallberg, 2007*). The synthesis was performed at 30 °C. After the ferrous iron oxidation and the precipitation the precipitate was harvested by centrifugation (6000 g, 15 min) and freeze dried. The samples will be called slow H_2O_2-schwertmannite. A third recipe was described by *Loan et al.* (2004) and samples were synthesized in a slightly modified way with 2.5 g of $Fe_2(SO_4)_3 \bullet xH_2O$ that was dissolved in 500 ml of MilliQ water in glass bottle and stored at 85 °C for 24 hours. The precipitate was vacuum dried and this sample will be referred to as 85 °C-schwertmannite.

2.3.2. XAS

XAS experiments were conducted at the SUL-X beamline at ANKA synchrotron facility in Karlsruhe, Germany. The investigated samples were synthesized by the dialyses bag method described above but initial solutions were modified by addition of arsenate, chromate or vanadate to replace sulfate. Samples were prepared with concentrations of 1.65 mmol (16.5 %), 2.5 mmol (25 %), 5 mmol (50 %) and 10 mmol (100 %), respectively, the percentage indicates the ratio of heavy metal to sulfate. Goethite and lepidocrocite samples were synthesized as references and exposed to solutions of arsenate, chromate or vanadate respectively. The solutions for the chromate standards contained 0.7 mM, 2 mM and 10 mM chromate, 1 mM and 5 mM arsenate and 1 mM vanadate, respectively.

2.3.3. Density functional theory (DFT) calculations

Using systematic density functional theory (DFT) calculations we study the structural, energetic, and sorption properties of schwertmannite as well as goethite(101), akaganeite(100), and lepidocrocite(010) surfaces with different terminations. The exchange and correlation potential is treated within the LDA/GGA+U approach which is explicitly suitable for the strongly correlated FeOOH system.

2.4. Schwertmannite Transformation and Arsenic Adsorption

2.4.1. SchwertmanniteTranformation tests

Stability experiments were carried out for four months using 5 g/L (equivalent to 7.75 mmol/L SO_4^{2-}) sediment load in milli-Q water using polypropylene reactor vials with regular shaking (4-5 times per day) at room temperature and atmospheric pressure. The system was investigated at four different pH conditions, i.e., 5.0, 6.0, 7.0 and 8.0. The pH adjustments were done with NaOH/HCl prior to addition of schwertmannite samples. Due to release of protons in the course of ageing processes (equation 2), additional pH adjustments were done daily using 1.0 N NaOH and the amount of NaOH consumed was noted. Samples were collected at regular intervals for four months. Similar stabilization experiments were conducted at pH 3.0, i.e., within the stability range of schwertmannite (pH 3-4.5) to distinguish the role of higher pH on the fate of sulfate. The solid phase was separated by filtration and oven dried at 60 °C.

2.4.2. As(III)-Schwertmannite interactions

Three different schwertmannite (SHM) specimens produced through chemical and biological processes were used in the current study. SHM_MS was synthesized in a mine water treatment plant (GEOS, Freiberg, Germany) by microbial oxidation of Fe(II) between pH 2.9-3.2 (*Glombitza et al., 2007*) from SO_4^{2-} rich mine waters. One schwertmannite sample was synthesized by fast synthesis method called »oxidative synthesis« as described by *Regenspurg and Peiffer* (2005). 10 g of $FeSO_4.*7H_2O$ was dissolved in deionized water and ~ 5 ml of 32% H_2O_2 was added drop wise to accelerate the oxidation of Fe^{2+} to Fe^{3+}. The reaction was preceded for 24 hours and the pH remained stable at 2.4. The precipitated orange coloured solids were filtered and oven dried at 35-40 °C. The samples were used directly for further experimental purposes without any treatment, cal-

led here after SHM_FS. Schwertmannite was also synthesised as described by *Bigham et al.* (1990) The specimen is called SHM_DS.

The sorption studies were conducted as batch experiments. The suspension was allowed to equilibrate for 5 days with a sediment load of 0.25 g/25 ml at pH 3.0 and initial As(III) concentrations ranging from 0.13 to 1.33 mmol/L. Preliminary kinetic experiments demonstrated that equilibrium is achieved after this time. The suspension was continuously stirred during the whole reaction time. The pH of the As(III) containing solutions were adjusted to pH 3.0±0.05 before addition of schwertmannite to avoid possible transformation of SHM at changing pH conditions (*Jönsson et al., 2005*). The ionic strength was maintained at 0.01 mol/L by $NaNO_3$. Experiments were performed in the dark in the presence of oxygen in polypropylene reactor vials that were preconditioned by 10 % nitric acid overnight. After the equilibration time samples were filtered through < 0.45 µm cellulose filter papers and the aqueous phase was analyzed for pH, Fe(II), Fe(t), SO_4^{2-} and As(t) concentrations. Solid phase was characterized by XRD, FTIR, SEM and XANES techniques. Solid phase arsenic loading was determined by mass balance ($CS=(C_i-C_{eq})*V/M$), where C_i and C^{eq} are initial and equilibrium As concentrations (mol/L), M is mass of sorbent (g), L is volume of solution (L). SHM samples were stored in crimp sealed serum vials in O_2 free glove box to eliminate the effect of atmospheric O_2 in As(III) oxidation during storage for As species measurement by XANES.

Two commonly used statistical isotherm models were fitted with experimental data using IsoFit v1.2 (*Matott and Rabideau, 2008*) to evaluate the sorption behavior. Langmuir model (Eq. 1) demonstrates a monolayer sorption mechanism with homogeneous sorption energies, while Freundlich model is an empirical model demonstrating multilayer sorption sites and heterogeneous sorption energies (Eq. 2) (*Weber and DiGiano, 1996*).

2.4.3. Dumping Experiments with Arsenic-loaded Schwertmannite/Transformation products

Long-term experiments were set up to study the development of the chemical bonding between the species and schwertmannite or schwertmannite transformation products upon ageing in order to test their deposition properties. Periodically, the desorption of arsenic by synthetic rainwater (pH 5, elution 1d/month, B-tests) or groundwater (pH 7, continuous elution, C-tests) was analysed. The »groundwater« was effluent water (< 0.1 mg As/L, <0.2 mg U/L) of the water treatment plant in Schlema-Alberoda (table 2). As summarized in table 5, five different »dumping sceniaros« were investigated. Each test contains 9g mineral precipitate and was eluted periodically or continuously by 10 mL water. The experiments will be accompanied by XAS (X-Ray-Absorption-Spectroscopy) and EXAFS studies, results were already open.

2.4.4. Laboratory experiments for pilot test preparation

Following to SHM transformation and As-Adsorption experiments from the last year, a other test was performed in duplicate. Therein, brown coal filter ash (FA) (co. the neutralization was used instead of the conventional dosage of lime milk. 1 L influent water from the water treatment plant in Schlema-Alberoda (average composition see table 2) was acidified by 0.1M HCl and air-stripped for 30 minutes in order to eliminate inorganic carbon. After filtration (0,2 µm cellulose acetate), FA (about 0.15 g/L as 0.5% FA-water suspension) and SHM (42.6 mg/L according to 20 mg Fe/L as 2 % SHM-water suspension) was added subsequently in order to distinguish between arsenic, uranium and radium immobilization to FA

$$c_s = c(s_{tot})\frac{K_{Ads}c_{eq}}{(1+K_{Ads}c_{eq})} \quad \text{(Eq.1)}$$

$$c_s = K_F \cdot C_{eq}^{\ n} \quad \text{(Eq.2)}$$

c_s = concentration of As(III) adsorbed at the solid phase (mol/g)
c_{eq} = equilibrium concentration of As(III) in the aqueous phase (mol/L)
$c(s_{tot})$ = total concentration of surface sites (mol/g)
K_{Ads} = Langmuir sorption coefficient (L/mol)
n = Freundlich exponent (≤ 1)
K_F = Freundlich adsorption coefficient (Ln/(moln-1 g))

Table 2: Selected parameters of the Schlema-Alberoda treatment plant's inflow (*May 2010*)

pH	redox potential	electric conductivity	Cl	SO_4	HCO_3	Fe(tot)	As	U	^{226}Ra
[-]	[mV]	[µS/cm]	[mg/L]						[mBq/L]
6,95	+/-0	2300	55	760	630	5	1.0	2.0	1700

Table 3: Overview of previously performed pilot test campaigns

Cam-paign	date	flow rate	schwermannite			pH-buffering agent
		m^3/h	sample	pre-conditioning	dosage (mg Fe/L)	
1	21.-23.10.09	0.5-0.75	S2-013	neutralized with lime milk	48	lime milk
2	10.-13.11.09	0.94-0.91	S2-013	neutralized with lime milk	25	lime milk
3	23.-26.11.09	0.93-0.88	S2-013	untreated	21	lime milk
4	09.-12.02.09	0.93	S2-015	untreated	(1.4)-36	lime milk
5	10.-19.03.10	0.90 – 0.70	S2-015	untreated	2.7 -25	lime milk
6a	06.-07.04.10	0.95	-	-	0 (blank)	lime milk
6b	07.-16.04.10	0.95 – 0.80	S2-001	untreated	9.8 - 22	lime milk
7	11.-20.08.10	1.00	S2-013	untreated	17-26	brown coal filter ash

and SHM. Samples were filtered by 0,2 µm cellulose acetate and acidified before AAS, ICP-OES as well as γ-spectrometry analysis.

2.5. Pilot test for removal of arsenic from mine water

The schwertmannite produced in the pilot plant Tzschelln was used to enhance the arsenic removal from mine water in the abandoned uranium mine of Schlema-Alberoda (East Germany). The uranium mine water has to be purified from iron, arsenic, uranium and radium, iron and manganese. The installed treatment technology is described by *Meyer, et al. (2009)*. The average composition of mine water inflow is shown in table 2.

The required limit of arsenic for discharging into the river Mulde is ≤ 0.1-0.3 mg/L (dependent on flow rate of the Zwickauer Mulde river). The naturally occurring iron concentration is not sufficient for complete arsenic removal or to meet the prescribed maximum value. Thus it was investigated, whether it is possible to enhance the arsenic removal by dosing SHM as a diluted aqueous suspension.
The pilot plant was constructed in a building of the mine water treatment plant of the Wismut at Schlema and consists of a precipitation tank, a flocculation tank and an inclined clarifier. A flow chart of the pilot plant is shown in figure 1. A data logger records the pH in the precipitation tank and enables adjustment of pH by controlling a peristaltic pump to dose lime milk. Table 3 summarized main parameters of the last seven pilot campaigns.

The water to be treated in the pilot plant is taken from the inflow of the mine water treatment plant after the acidification and CO_2 stripping stage.
Until now three schwertmannite samples were applied: two wet filtered aggregate samples and one dried sample from the pilot plant at Tzschelln. The schwertmannite is suspended in process water and stored in a tank with agita-

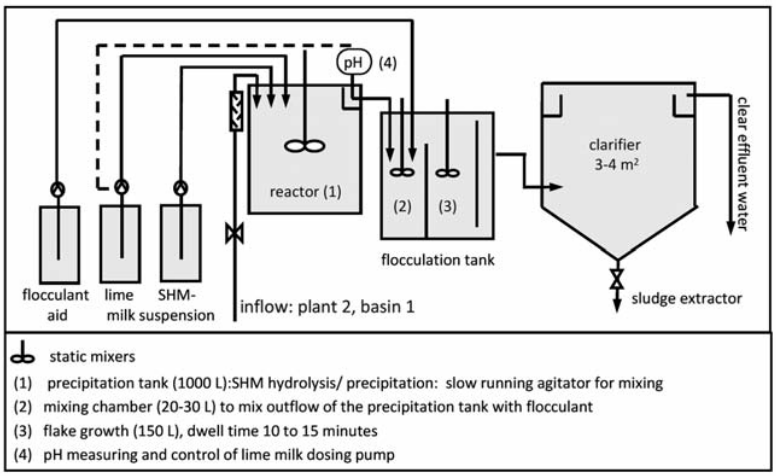

Figure 1: Flow chart of the mine water treatment pilot plant

tor. In the first pilot experiments the schwertmannite was pre-hydrolysized by adding lime milk to the storage tank until pH 8. Schwertmannite suspension with 5 wt% of solids led to plugging of the dosing tube. Dilution to 1 wt% solved the problem.

Lime milk and a flocculant are taken from the storage tanks of the mine water treatment plant. With a peristaltic pump the schwertmannite suspension is dosed into the precipitation tank. Lime milk is dosed simultanously to adjust pH to 7.5. Subsequently the water flows to the flocculation tank where the polymer flocculant is dosed. In this tank precipitates are transformed to flocks. In the following inclined clarifier these flocks are sedimented. The overflow of the clarifier goes back into the main treatment plant.

To monitor the treatment process inflow and outflow of the pilot plant were analyzed for total arsenic, iron and uranium. In the outflow, dissolved concentrations were determined, too. The sludge from the clarifier was analysed for uranium and arsenic and investigated by a sedimentation test.

3. Results and Discussion

3.1. Microbial Investigations

3.1.1. Bacterial activity and diversity in the schwertmannite deposits

For a stable process of schwertmannite generation the number and activity of iron oxidizing bacteria play a key role in the pilot plant. Because bacteria are present in the water as well as in the schwertmannite that is deposited on the carrier material a recirculation of precipitated schwertmannite could stabilize the process and increase the oxidation rate if the bacterial cell numbers are high in the mineral phase.

To obtain detailed information about the activity and diversity of bacteria in the schwertmannite a depth profile was prepared and the microbial cells were analysed with a Bacterial Viability Kit and FISH analyses. A 4-week old 2 cm thick sample core was cut into 4 layers, where layer 0-0.5 cm represented the youngest (water facing) layer.

The first data indicate a decreasing total cell number with increasing depth (Fig.2). $3x10^6$ cells were detected in the first layer (0-0.5 cm) and $1.4x10^6$ cells in the deepest layer (1.5-2.0 cm). More than 40 % of the cells in the first centimetre were found to be viable. In the deepest layer more than 30 % of the cells were still alive. This trend could be observed in material from different water depth.

To obtain information about the microbial community structure in the different layers the samples were investigated with FISH probes for *Ferrovum myxofaciens* and *Gallionella* TrefC4. Figure 3 shows the dominance of *Ferrovum myxofaciens* which reaches 25 to 36 % of the

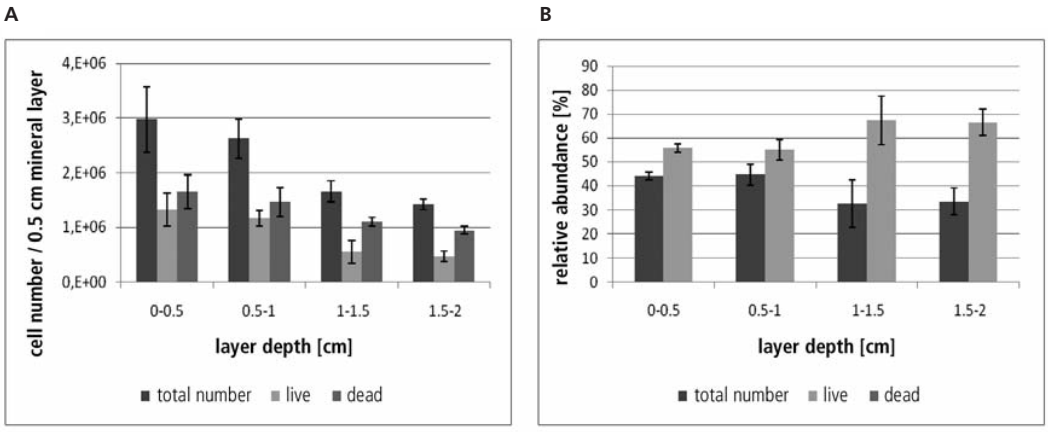

Figure 2: **A** cell number of total, living and dead cell per mineral layer, **B** relative abundance of living and dead cells in correlation to the depth of schwertmannite deposit on carrier material

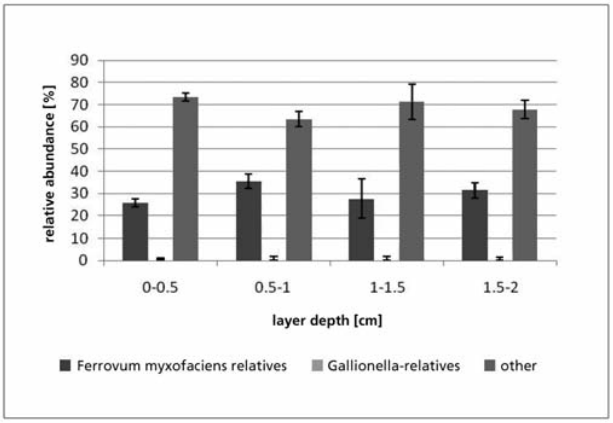

Figure 3: relative abundance of *Ferrovum myxofaciens* and *Gallionella* TrefC4 in correlation to the depth of schwertmannite deposit on carrier material

microbial community. In contrast to this approximately only 1% of the microbial cells were detected as *Gallionella* TrefC4 cells.

Previous investigations of the microbial community from water of the pilot plant demonstrated, that relatives of *Ferrovum myxofaciens* and *Gallionella* are the main species with a percentage of the total microbial community up to 90% (*Heinzel et al. 2009*).The differences may be due to the use of different methods for the analyses. For example T-RFLP, used by *Heinzel et al.* (2009), analyses the relative composition of PCR-amplified 16S rRNA gene fragments. In contrast to this, the microscopic FISH approach to quantify cells by fluorescent DNA probe is a direct method that avoids the PCR amplification. PCR amplification has been shown to produce artifacts in microbial diversity (*Acinas et al. 2005*).

This problem of comparison between FISH-based and PCR-based analyses is also supported by our initial results from first TRFLP analyses of the same samples that indicate that *Ferrovum myxofaciens* comprises up to 90% of the total bacterial cells (data not shown). More analyses have to been done to quantify the microbial diversity and activity and to give a suggestion which part of the schwertmannite deposit should recirculate.

3.1.2 Biologic Analysis / Interface Bacteria – Mineral

Ferris et al. (2004) put forward the theory that schwertmannite hedge hogs (globular aggregates with concentrically surrounded by schwertmannite whiskers) are overgrown bacteria. Our TEM analyses of microtome sections showed that these hedge hogs are in fact massive and that no sign of overgrown cells are in inside these aggregations (Fig. 4). Furthermore no direct connection of bacteria and mineral could be found. Instead traces of EPS (extra-

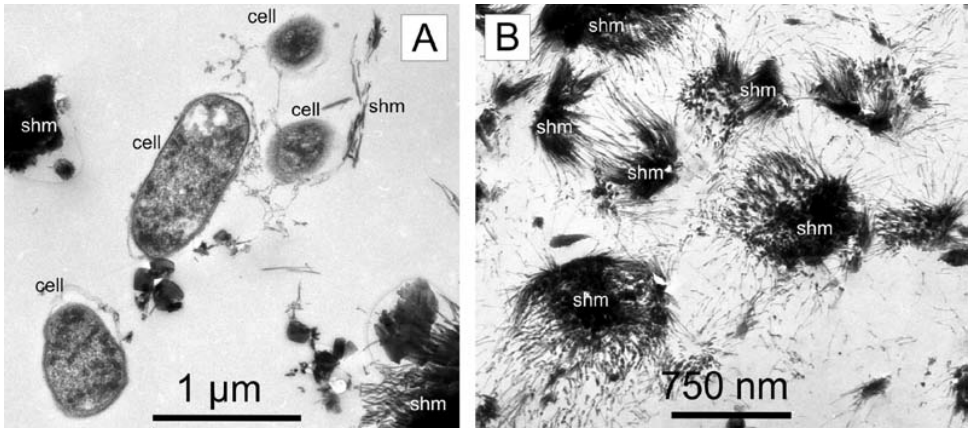

Figure 4: TEM images from cultures of *Leptospirillum ferrooxidans*. **A** Two cells that are surrounded by EPS. The schwertmannite whiskers in that sample are not connected directly to the cell but to the EPS. **B** Sections through schwertmannite hedge hogs. They are of massive nature and no signs of an overgrown cell can be found in the center

cellular polymeric substance) are present in the samples that connect mineral and cell. We assume that the EPS is a seed for the precipitation of schwertmannite to prevent lethal cell overgrowth. This hypothesis is underlined by the results of section 3.3.2. where we show that schwertmannite whiskers form if the oxidation of iron happens slowly, irrespective of a biotic or abiotic environment.

3.2. Schwertmannite Generation: Estimation of the oxidation capacity

The microbially enhanced oxidation process in the pilot plant occurs both on the surface of the biofilm carriers and in the free volume of the oxidation basin. The oxidation rate is influenced by various parameters, e.g. oxygen supply, pH, temperature, sludge circulation, composition of the inflowing mine water and surface area of the biofilm carrier. At technical scale only the sludge circulation and the amounts of carriers can be used to accelerate the oxidation rate. So in a first step the oxidation rate was determined in the pilot plant at different surface areas of the growth carrier. In these experiments the oxidation rate was calculated according to Eq. (3) from the total amount of ferric iron (Fe(III)ges) formed during microbial oxidation and the residence time τ. The results are presented in figure 5. By drawing the oxidation rate as a function of A_F/V_R ratio it was possible to distinguish $\nu_{Ox\text{-}F}$ and $\nu_{Ox\text{-}V}$ and to estimate these values.

Fig. 6 shows the oxidation rate of the pilot plant according eq. (1). Oxidation rates in the range of 10 – 40 g/(m³h) were achieved. The overall value was in the range of 20 – 25 g/(m³h).

$$\nu_{ox} = \frac{Fe(III)_{ges}}{\tau} = \frac{Fe(III)_{ges}}{v_R} \cdot Q_{zu} = \nu_{ox-F} \cdot \frac{A_F}{V_R} + \nu_{ox-V} \quad \left[\frac{g}{m^3 \cdot h}\right] \qquad \text{(Eq.3)}$$

(Eq.3)

A_F	Surface of the growth carriers and all other surfaces inside the reactor	[m²]
$Fe(III)_{ges}$	Total amount of ferric iron formed by microbial oxidation	[g/m³]
Q_{Zu}	Inflow	[m³/h]
V_R	Reactor volume	[m³]
ν_{Ox}	Total (overall) oxidation rate	[g/(m³·h)]
$\nu_{Ox\text{-}F}$	Oxidation rate caused by oxidation at the carrier	[g/(m²·h)]
$\nu_{Ox\text{-}V}$	Oxidation rate caused by oxidation in free reactor volume	[g/(m³·h)]

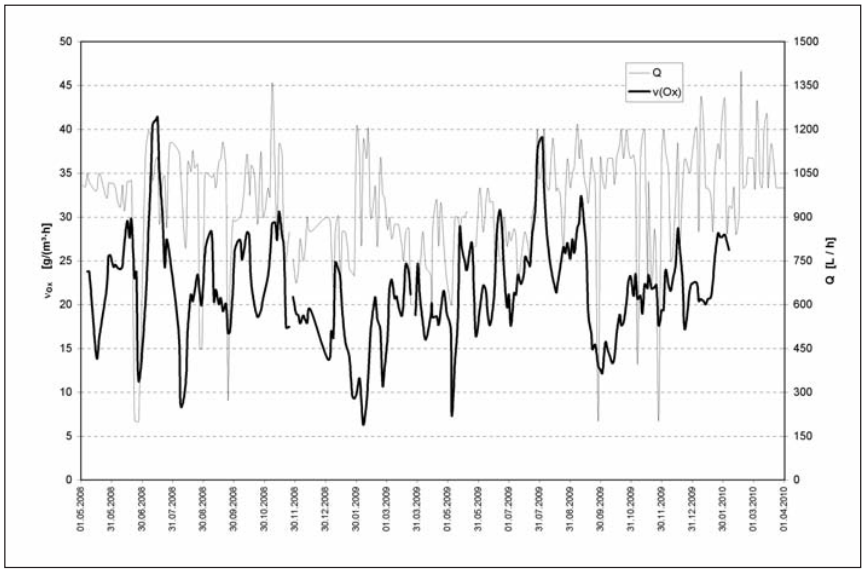

Figure 6: Oxidation rate and throughput of the pilot plant at Tzschelln until April 2010

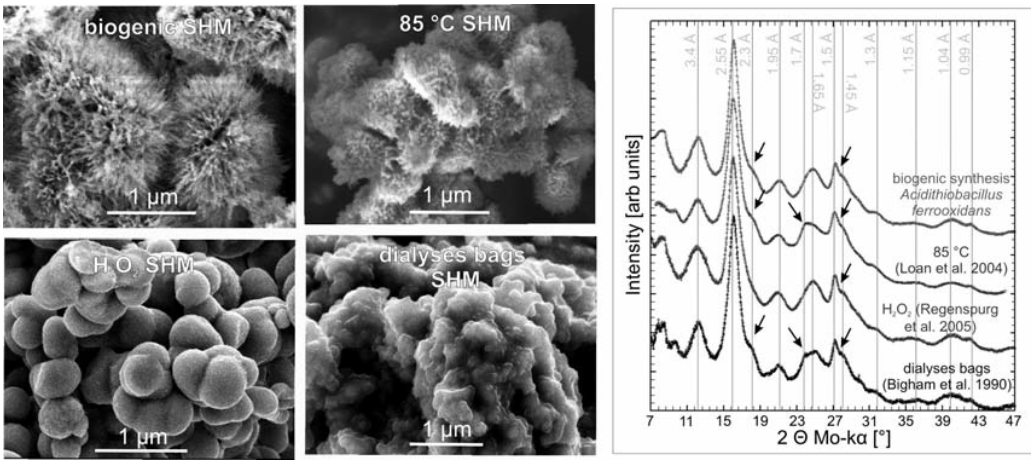

Figure 7: Left: Exemplary SEM pictures of schwertmannite precipitated by different methods. The typical schwertmannite hedge hog morphology is present in the biogenic schwertmannite (produced in the pilot plant) and the schwertmannite synthesized abiotically at 85 °C. Right: diffractograms of synthesized samples. All show the typical schwertmannite reflections, however, the products differ regarding the intensity ratio between several peaks (e.g. 1.5 Å vs. 1.45 Å, intensity of shoulder at 2.3 Å) as well as regarding the peak width.

The influence of the flow-rate on the oxidation performance of the pilot plant was discussed in detail in the Science Report 2009 (*Peiffer et al., 2009*).

3.3. Mineralogical and Structural Analysis

3.3.1. Schwertmannite structure

The morphology of the schwertmannite depends on the way of synthesis. Samples that were synthesized with H_2O_2 consist of round spheres whereas samples that were produced by bacterial oxidation showed the characteristic whiskers. Samples synthesized in an inorganic but slow way showed a third variety. Exemplary SEM pictures are shown in Fig. 7. Samples synthetised by a slow oxidation with diluted H_2O_2 also showed whiskers indicating that the whiskers form in environments with slower oxidation processes and not specifically

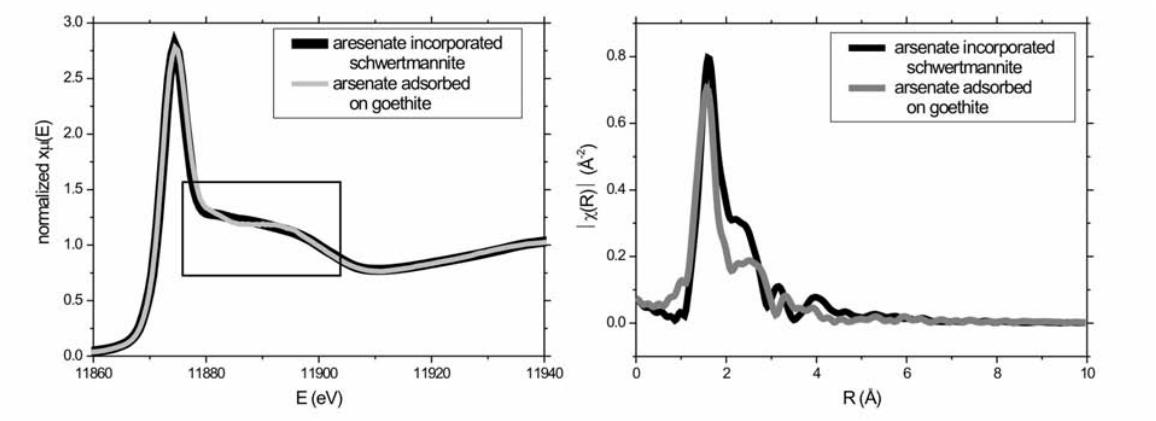

Figure 8: Representative examples of As K-edge EXAFS spectra of representative examples of aresenate adsorbed on goethite (grey) and incorporated in schwertmannite (black). The left graph shows a magnification of the XANES region. Please note the differences between goethite and schwertmannite in the marked box. The graphs on the right show the radial distribution function. Whereas the first coordination sphere (As-O) is the same in both samples the second (shoulder between 2 and 3 Å) and third (between 3 and 4 Å) coordination sphere is closer to the central atom indicating a stronger bond.

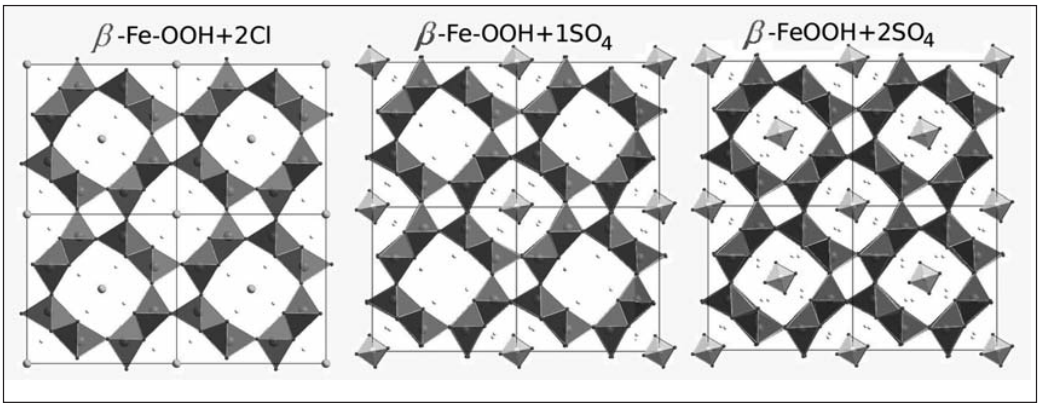

Figure 9: Akaganeite with interstitial ions

due to biotic/organic influence. The XRD measurement on the 2D detector allowed precise analyses of the different synthesized schwertmannites in finite time. Even though the specimens show similar diffraction patterns there are distinct variations in intensity and peak width. Also additional reflections appear in some samples (Fig. 1). This indicates that the »schwertmannites« are not one homogeneous phase but a mixture. This raises the demand for a reproducible method to synthesize pure schwertmannite.

3.3.2. XAS

The evaluation of XAS data is ongoing work. Preliminary results on the As K-edge spectra of arsenic adsorbed to lepidocrocite and goethite are essentially identical independent of As concentration and of the adsorbant. Also the As K-edge spectra of schwertmannite are identical for different concentrations of As. Anyhow, a comparison of the spectra and the radial distribution function of both materials, the standards and the co-precipitated schwertmannites, shows that arsenate absorbed in schwertmannite is bonded more closely, and therefore more strongly, to the iron than the arsenate adsorbed on goethite and lepidocrocite surfaces (Fig. 8).

3.3.3. Results DFT: Bulk FeOOH polymorphs and bulk schwertmannite

Our work on the bulk properties of the FeOOH polymorphs goethite (α), akaganeite (β), lepi-

docrocite (γ), and the high pressure phase (ε) was recently published in Physical Review B (*Otte 2009*). The energetic relations among the phases reveal that the framework structures (α, β, ε) are more favorable than the layered one (γ). The schwertmannite structure is considered akin to akaganeite where additional interstitial sulfate ions are added in the channels, see Fig. 9. Because schwertmannite is synthesized in Cl- containing solution, we consider as a starting point Cl atoms in the akaganeite channels. We find that the Cl-ions widen the channels. As Cl is singly negatively charged, we have explored the role of introducing a background charge of the whole simulation cell to model correctly the electronic properties.

Table 4:

β-FeOOH+	**1SO_4**	**2Cl**	**2SO_4**
V_0 [Å^3/f.u.]	42.54 [+1%]	42.33 [+0.5%]	42.96 [+2%]
$E_{sorption}$[eV]	-0.195	-0.265	-0.092

Furthermore, we explore the bonding mechanisms of SO_4^{2-}. We find that the channels adapt to the ions in the middle of the channels. However, this adjustment of the framework is connected with a high energy cost. The sorption energy of the system can be determined per formula unit and unit cell (f.u./u.c.) as

$$E_{Sorption}=E_{System}-E_{\beta\text{-}FeOOH}-E_{Ion} \quad \text{(Equ.4)}$$

where negative values correspond to an exothermic reaction. The absolute value sorption energy decreases with increasing sulfate concentration: The lowest absolute value of $E_{Sorption}$ =-0.092 eV is obtained fort the highest sulfate concentration (every akaganeite channel is occupied by sulfate ions) where the strongest distortion of the akaganeite framework occurs (table 4). The sum formula of schwertmannite Fe16O16(OH)16-2n(SO4)n (n=1-3) according to (Bigham 1994) allows for an even higher sulfate concentration in exchange with hydroxyl groups. Therefore, further bonding mechanisms (mono- and bidentate) are currently under investigation.
A further task under investigation is the sorption of As(V). As an even larger molecule, it is found to cause a stronger distortion of the framework. The sulfate-arsenate exchange is a further aspect we are currently working on.

Sorption on the FeOOH surfaces

The FeOOH polymorphs have high surface areas and high sorption affinities for aqueous solutes (*Cornell 2001*). The transformation product after arsenate incorporation in schwertmannite is expected to be a FeOOH polymorph. Various terminations of the most prominent and relevant surfaces in sorption reactions, goethite(101), akaganeite(100), and lepidocrocite (010), are modeled. Prior to studying adsorp-

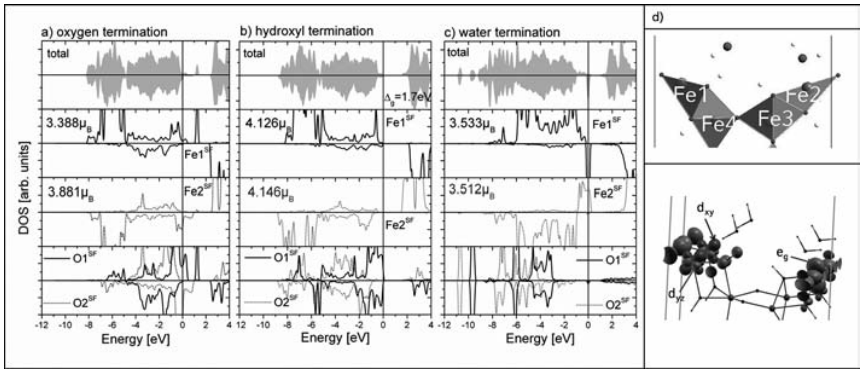

Figure 10: Density of states (a-c) and spin density plot (d) of β-FeOOH (100)-surface

tion processes it is important to understand the properties of the clean surfaces. Oxygen, hydroxyl and water terminations are considered to model different pH conditions.

Indeed, we find that the surface termination impacts strongly the oxidation state of the Fe at the surface as displayed in Fig. 10 for akaganeite(100). The deprotonated oxygen termination (basic condition, Fig. 10a) leads to a reduction of the surface iron, Fe^{SF}, and the respective magnetic moments, MFe, are reduced. The hydroxyl termination with all iron in Fe^{3+} and a band gap of 1.7eV (Fig. 10b) is closest to bulk behavior. For a water termination which represents an acid environment, (Fig. 10c), the Fe^{SF} are reduced to Fe^{2+} and a breaking of FeO_6 octahedra at the surface occurs.

The spin density plot (Fig. 10d) integrated around the Fermi level for the water termination reveals that the $Fe1^{SF}$ is reduced with a 6^{th} partially occupied d_{xy} orbital, while for $Fe2^{SF}$ the one spin channel is fully and a 6^{th} electron appears in the opposite spin channel with partially filled e_g-states at the Fermi level. Similar properties are obtained for goethite(101) and lepidocrocite(010), but are not displayed here. Ongoing work focuses on the adsorption of arsenate on these relaxed surface terminations.

3.4. Schwertmannite Transformation and Arsenic Adsorption

3.4.1. Transformation of schwertmannite

Long term exposure of schwertmannite to pH values between 5 and 8 for 4 months at normal atmospheric condition leads a sulfate release, which increased with time and pH up to roughly 1.40 mmol/g solid phase, corresponding to 90 % of total initial sulfate, after 4 months of exposure at pH 8 (Fig.11). The higher SO_4^{2-} release at elevated pH is probably due to the direct exchange of OH^- for the SO_4^{2-} ion at the schwertmannite surface, while faster SO_4^{2-} release during initial days may be due to release of surface-adsorbed SO_4^{2-}.

3.4.2. As(III)-schwertmannite interactions

A detailed understanding on As(III)-schwertmannite interaction in acidic medium which will foster attempts to remove As(III) with this mineral was obtained. Schwertmannites turned out to be able to remove significant fractions of As(III) (> 97 %) from contaminated water, the efficiency of which strongly depends on surface area and synthesis pathway. The different synthesis products, produced through biotical and abiotical synthesis pathways differ in their physical and chemical properties including morphology, dissolution rate, surface area and crystallinity which strongly affects the

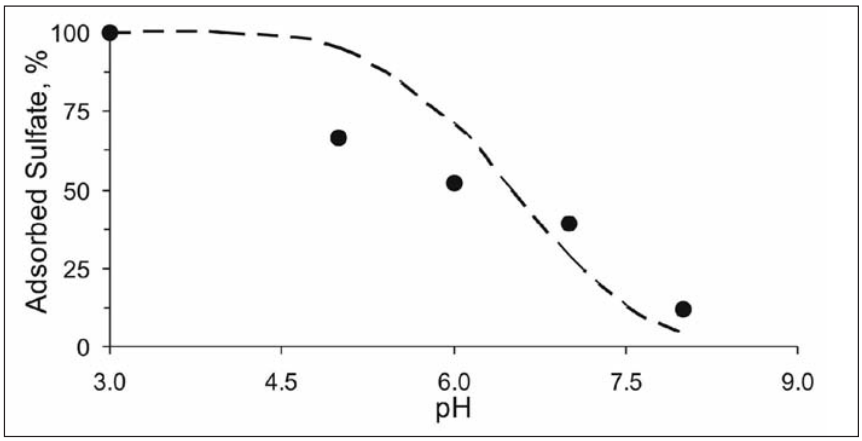

Figure 11: PHREEQC modelled (lines) SO_4^{2-} adsorption profile by schwertmannite at different pH values. The experimentally observed values at pH 5, 6, 7 and 8 after 120 days are shown as filled circles.

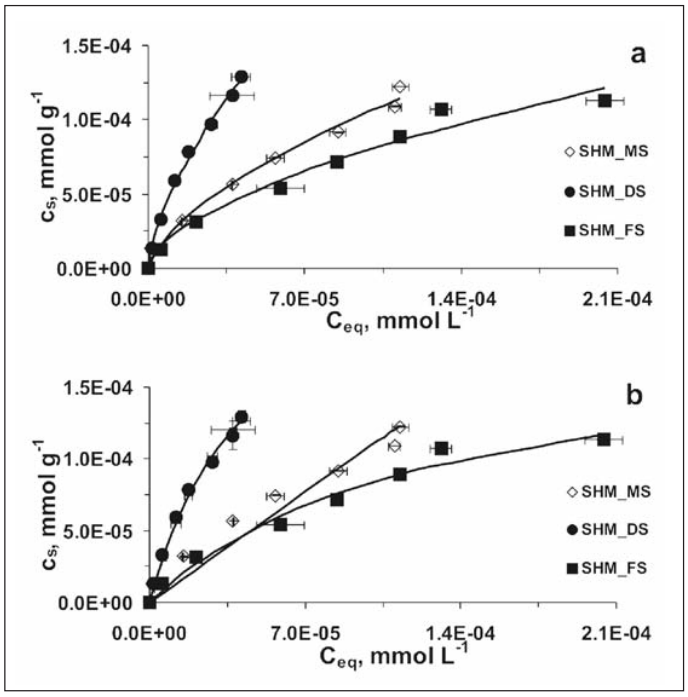

Figure12: Freundlich (a) and Langmuir (b) sorption model fits to the experimental data. Solid lines repre-sent model predicted sorbed As(III), while experimental data are shown by filled and open symbols.

Table 5: Arsenic mobilization under different dumping scenarios

Scenario	1 (blank)		2 (blank)		3		4		5	
	dumping of uncontamined SHM		dumping of un-contamined SHM-transformation product		dumping of **As** loaded **SHM**		dumping of **As** loaded **SHM transformation product**		dumping of **As** and **U** loaded **SHM transformation product**	
As adsorbed (mol As/ mol SHM)	0.00016		0.00016		0.02535		0.02557		0.02250	
test	**1B**	**1C**	**2B**	**2C**	**3B**	**3C**	**4B**	**4C**	**5B**	**5C**
arsenic elution by / time	rainwater (pH 5) 1d/month	ground-water (pH 7)	rainwater (pH 5) 1d/month	ground-water (pH 7)	rainwater (pH 5) 1d/month	ground-water (pH 7)	rainwater (pH 5) 1d/month	ground-water (pH 7)	rainwater (pH 5) 1d/month	ground-water (pH 7)
49 d	0.24%	0,00%	0,17%		**1.38%**	0.07%	0,02%	0,00%	0,00%	0,00%
78 d	0,17%	0,00%	0,00%	0,00%	**1.00%**	0,05%	0,02%	0,00%	0,00%	0,00%
106 d	0,00%	0,00%	0,07%	0,00%	**1.22%**	0,04%	0,02%	0,00%	0,00%	0,00%
140 d	0,09%	0,00%	0,06%	0,00%	**1,44%**	0,02%	0,02%	0,00%	0,00%	0,00%

sorption behaviour of As(III) (Fig.12).

Our findings suggests the occurrence of two removal mechanisms: 1) ligand exchange with surface adsorbed SO_4^{2-} which appears to be of minor relevance as indicated by the absence of any particular trend in SO_4^{2-} release in case of SHM_FS, and the weak SO_4^{2-} release in case of SHM_DS inspite the highest As(III) uptake and SSA of the three specimens and 2) formation of amorphous As(III)-Fe(III)-SO_4^{2-} precipitates at higher aqueous As concentrations as indicated by increased diffraction intensity proportionally with the As(III) loading and the appearance of new IR bands. These amorphous surface precipitates may stabilize sorbed As(III) towards surface oxidation. Most of the aqueous As(III) appeared to sorb through the second mechanism.

3.4.3. Dumping experiments with As-loaded SHM – samples

The relative amounts (%) of mobilized arsenic by periodical eluation with rain water (pH 5, B-

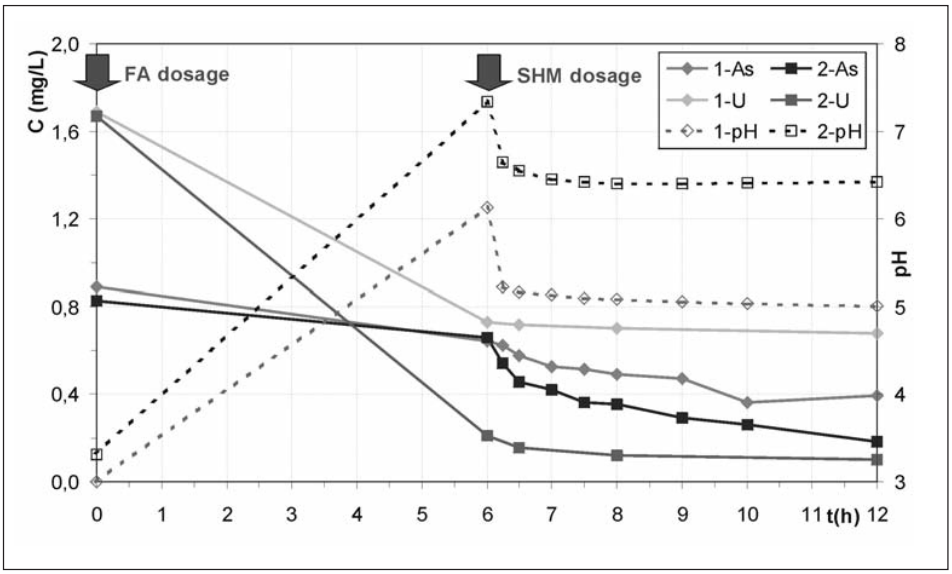

Figure 13: Arsenic and uranium elimination in batch tests, where FA was used as neutralizing agent

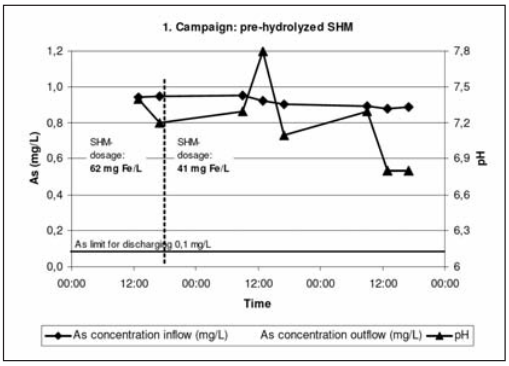

Figure 14: Comparison of As concentration of inflow and outflow (pre-hydrolyzed SHM, 62 and 41 mg Fe/L)

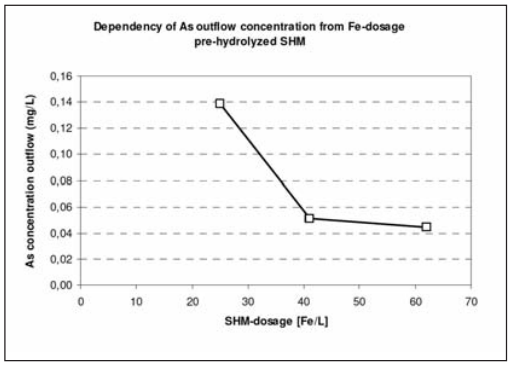

Figure 15: Residual As concentration depending from SHM dosage (pre-hydrolyzed SHM)

tets) or continuous elution with groundwater (pH 7) were summarized in table 5. Actually (after 140 days), a significant arsenic mobilization was only detectable in test 3B, a periodical elution of As-loaded Schwertmannit with rain water.

3.4.4. Laboratory experiments for pilot test preparation

Fig. 13 shows the promising results of the first batch tests, where brown coal filter ash (FA) was used instead of lime milk for the neutralisation of the acidic process water of the water treatment plant in Schlema-Alberoda. Six hours after the addition of 0.21 g/L (test 1) and 0.16 g/L (test 2) FA addition, 0.22 mg As/L and 0.96 mg U/L could be immobilized in test 1 (pH6,13), 0.17 mg As/L and 1.46 mg U/L in SHM/L (20 mg Fe/L) was added to each test. Six hours later, a total of 0.49 mg As/L, 1.01 mg U/L and about 1000 mBq ^{226}Ra/L were eliminated in test 1 (pH 5.01), a total of 0.64 mg As/L, 1.57 mg U/L and about 930 mBq ^{226}Ra/L in test 2 (pH 6.42).

3.5. Pilot test for removal of arsenic from mine water

As mentioned above the required limit of As for discharging into the river Mulde is ≤ 0.1 0.3 mg/L (dependent on flow rate of the Zwickauer Mulde river). The naturally occurring iron concentration is not sufficient for complete arsenic removal or to meet the prescribed maximum

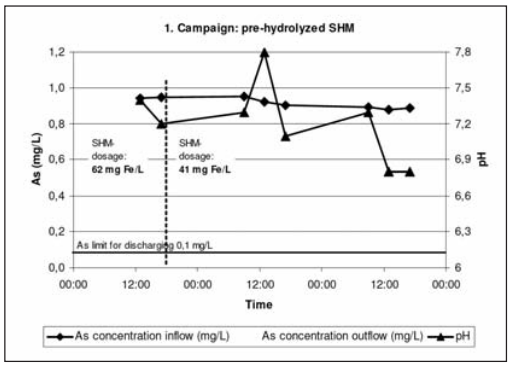

Figure 16: Comparison of As concentration of inflow and outflow (untreated SHM, 21 mg Fe/L)

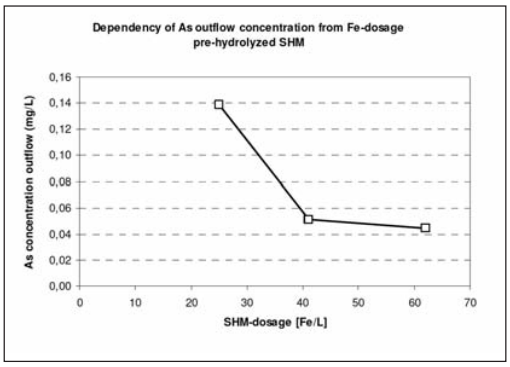

Figure 17: Enhancement of arsenic removal by dosage of schwertmannite suspension

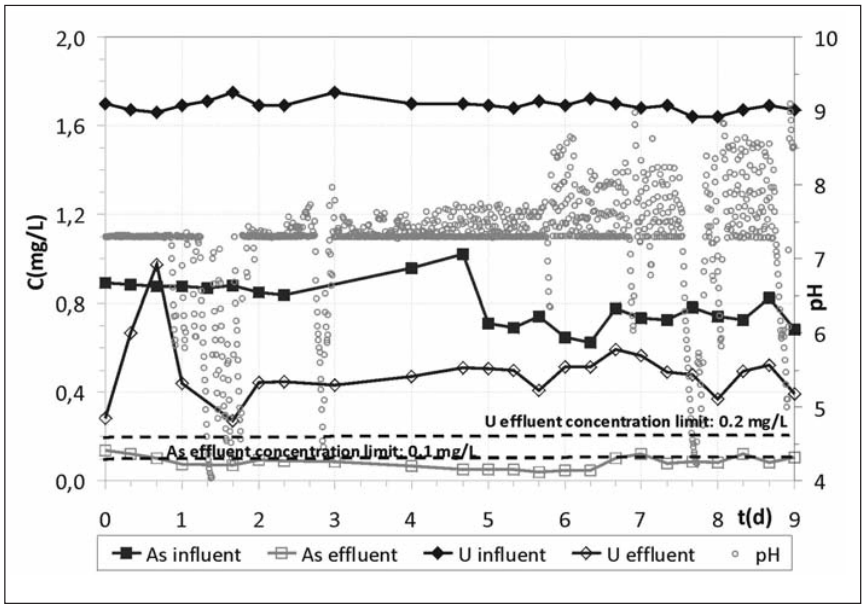

Figure 18: Arsenic and Uranium elimination during the pilot test campaign 7

value. The main results of the pilot tests are shown in fig. 14 to 17. Fig. 14 shows the results of the first pilot experiment with pre-hydrolyzed SHM. Pre-hydrolysis was applied because lab scale investigations of the revealed that the SHM transformation at high sulfate concentrations, as in the Schlema-Alberoda mine water, is delayed. In order to directly compare the performance of the two SHM varieties in the third pilot experiment untreated SHM was applied (fig. 16).

Surprisingly in the campaign with untreated SHM at comparable dosage a better As elimination was obtained. A dosage >30 mg Fe/L pre-hydrolyzed SHM was necessary to reach the limit for discharge of 0.1 mg As/L (Fig.15). With untreated SHM dosage of 21mg Fe/L was sufficient to reach this concentration. Fig 17 shows that, compared to As removal by the iron content of the mine water alone, it was possible to improve the arsenic removal from 60 % to nearly 90 % by dosing 20-40 mg/L Fe, and 35-70 mg/L SHM (dry mass) respectively.
Following to the promising results of the first batch tests with brown coal filter ash (FA) as neutralizing agent (chapter 3.4.4),pilot test campaign 7 was performed with FA dosage instead of lime milk. A suspension of 5 % FA and water of the river Mulde was used. This leads to an average, effective dosage of 0,15 g FA/L process water. The SHM-addition was

comparable with the foregoing campaigns (17-26 mg Fe/L). As shown in Fig.18, the required limit for discharging into the river Mulde could always be hold for arsenic. The averaged uranium elimination was 1,2 mg/L, probably due to a precipitation of Calciumuranate together with eluated Calcium from the FA.

4. References

Acinas, S. G., Sarma-Rupavtarm, R., Klepac-Ceraj, V. and Martin F. Polz (2005): PCR-Induced Sequence Artifacts and Bias: Insights from Comparison of Two 16S rRNA Clone Libraries Constructed from the Same Sample. Appl. Environ. Mircobiol 71:8966-8969.

Bigham et al., (1994) Mineral. Mag. 58: 641

Bigham, J. M., Schwertmann, U., Carlson, L., Murad, E. (1990): A poorly crystallized oxyhydroxysulfate of iron formed by bacterial oxidation of Fe(II) in acid mine water. Geochimica et Cosmochimica Acta, 54, 2743-2758.

Brunauer, S., P.H. Emmett and E. Teller (1938): Adsorption of gases in multimolecular layers. J. Am. Chem. Soc. 60: 309-19

Cornell and Schwertmann, (2001): Wiley-VCH GmBH & Co. KGaA, Weinheim, ISBN 3-527-30274-3

Ferris F. G., Hallbeck, L., Kennedy, C.B., Pedersen, K. (2004): Geochemistry of acidic Rio Tinto headwaters and role of bacteria in solid phase metal partitioning. Chemical Geology, 212, 291-300.

Glombitza, F., Janneck, E., Arnold, I., Rolland, W., Uhlmann, W.(2007): Eisenhydroxisulfate aus der Bergbauwasserbehandlung als Rohstoff. In: Heft 110 der Schriftenreihe der GDMB, S.31-40 ISBN 3-935797-35-4

Hallberg, K.B., K. Coupland, S. Kimura and D.B. Johnson (2006): Macroscopic streamer growths in acidic, metal-rich mine waters in north Wales consist of novel and remarkably simple bacterial communities. Appl. Environ. Mircobiol. 72(3): 2022-2030

Heinzel, E., E. Janneck, F. Glombitza, M. Schlömann and J. Seifert (2009): Population dynamics of iron-oxidizing communities in pilot plants for the treatment of acid mine waters. Environ. Sci. Technol. 43(16): 6138-6144

Janneck, E., (2008) Abschlussbericht FKZ: 01 RI05013; Teilprojekt 1: Koordination sowie Anlagenbetrieb und Produktherstellung

Loan, M., Cowley, J. M., Hart, R., Parkinson, G. M. (2004): Evidence on the structure of synthetic schwertmannite. American Mineralogist, 89, 1735-1742.

Otte, K., Pentcheva, R., Schmahl, W. W. and Rustad, J. R.; (2009): Pressure induced structural and electronic transitions in FeOOH from first principles, Phys. Rev. B 85, 205116

Peiffer, S., Burghardt, D., Janneck, E., Pinka, J., Schlömann, M., Wiacek, C., Seifert, J., Schmahl, W., Pentcheva, R., Meyer, J., Rolland, W. (2008) in: Geotechnologien Science Report No. 12, pp. 34-45; ISSN 1619-7399

Regenspurg, S., Peifer, S. (2005): Arsenate and chromate incorporation in schwertmannite. Applied Geochemistry, 20, 1226-1339.